Sports Medicine and Health Science 6 (2024) 344–357

Contents lists available at ScienceDirect

Sports Medicine and Health Science

journal homepage: www.keaipublishing.com/smhs

Research Article

Aerobic interval training preconditioning protocols inhibit isoproterenol-induced pathological cardiac remodeling in rats: Implications on oxidative balance, autophagy, and apoptosis

Hakimeh Shahsavarnajand Bonab [a], Javad Tolouei Azar [a,1,*], Hamid Soraya [b,1,**], Akbar Nouri Habashi [a]

[a] Department of Exercise Physiology and Corrective Exercises, Faculty of Sport Sciences, Urmia University, Urmia, Iran
[b] Department of Pharmacology and Toxicology, School of Pharmacy, Urmia University of Medical Sciences, Urmia, Iran

ARTICLE INFO

Keywords:
Pathological cardiac remodeling
Aerobic interval training preconditioning
Oxidative stress
Autophagy
Apoptosis

ABSTRACT

This study aimed to investigate the potential cardioprotective effects of moderate and high-intensity aerobic interval training (MIIT and HIIT) preconditioning. The focus was on histological changes, pro-oxidant-antioxidant balance, autophagy initiation, and apoptosis in myocardial tissue incited by isoproterenol-induced pathological cardiac remodeling (ISO-induced PCR). Male Wistar rats were randomly divided into control ($n = 6$), ISO ($n = 8$), MIIT ($n = 4$), HIIT ($n = 4$), MIIT + ISO ($n = 8$), and HIIT + ISO ($n = 8$) groups. The MIIT and HIIT protocols were administered for 10 weeks, followed by the induction of cardiac remodeling using subcutaneous injection of ISO (100 mg/kg for two consecutive days). Alterations in heart rate (HR), mean arterial pressure (MAP), rate pressure product (RPP), myocardial oxygen consumption ($M\dot{V}O_2$), cardiac hypertrophy, histopathological changes, pro-oxidant-antioxidant balance, autophagy biomarkers (Beclin-1, Atg7, p62, LC3 I/II), and apoptotic cell distribution were measured. The findings revealed that the MIIT + ISO and HIIT + ISO groups demonstrated diminished myocardial damage, hemorrhage, immune cell infiltration, edema, necrosis, and apoptosis compared to ISO-induced rats. MIIT and HIIT preconditioning mitigated HR, enhanced MAP, and preserved $M\dot{V}O_2$ and RPP. The pro-oxidant-antioxidant balance was sustained in both MIIT + ISO and HIIT + ISO groups, with MIIT primarily inhibiting pro-apoptotic autophagy progression through maintaining pro-oxidant-antioxidant balance, and HIIT promoting pro-survival autophagy. The results demonstrated the beneficial effects of both MIIT and HIIT as AITs preconditioning in ameliorating ISO-induced PCR by improving exercise capacity, hemodynamic parameters, and histopathological changes. Some of these protective effects can be attributed to the modulation of cardiac apoptosis, autophagy, and oxidative stress.

1. Introduction

Despite advancements in medical treatments, the mortality rates linked to cardiac remodeling and dysfunction remain high.[1] The term "remodeling" has been used to describe various clinical conditions and pathophysiological changes. In 2000, an international forum defined cardiac remodeling as molecular, cellular, and interstitial changes that lead to changes in the size, shape, and function of the heart due to cardiac injury. The forum identified two types of cardiac remodeling - physiological (adaptive) and pathological. The study specifically discusses the detrimental, pathological cardiac remodeling.[2] Isoproterenol (ISO), a synthetic β-adrenoceptor agonist, has been widely accepted as an inducer of cardiac remodeling in experimental animals.[1] The administration of ISO, which is known to elevate the heart rate and deplete the energy reserves of myocytes, presents a significant pathological challenge to the heart.[3] This challenge is capable of triggering a multitude of cellular mechanisms. Interestingly, these mechanisms are also observed in spontaneous or experimentally induced myocardial infarction (MI). ISO-induced PCR involves injury, necrosis, cardiac apoptosis and disruption of energy reserves in cardiomyocytes (CMs), leading to cardiac dysfunction.[1,4] The necrosis of CMs leads to increased membrane

* Corresponding author. Department of Exercise Physiology and Corrective Exercises, Faculty of Sport Sciences, Urmia University, Urmia, Iran.
** Corresponding author. Department of Pharmacology and Toxicology, School of Pharmacy, Urmia University of Medical Sciences, Urmia, Iran.
E-mail addresses: j.tolouei azar@urmia.ac.ir (J. Tolouei Azar), soraya.h@umsu.ac.ir, hamid_soraya2000@yahoo.com (H. Soraya).
[1] Contributed equally.

https://doi.org/10.1016/j.smhs.2024.01.010
Received 2 August 2023; Received in revised form 23 January 2024; Accepted 31 January 2024
Available online 2 February 2024

Abbreviations

MI	myocardial infarction
CMs	cardiomyocytes
ATP	adenosine triphosphate
IR	ischemia-reperfusion
EP	exercise preconditioning
IP	ischemic preconditioning
Smax	maximum running speed
AIT	aerobic interval training
TAC	total antioxidant capacity
TOS	total oxidant status
MIIT	moderate intensity interval training
HIIT	high-intensity interval training
ISO	isoproterenol
ISO induced PCR	ISO induced pathological cardiac remodeling
HR	heart rate
ABP	arterial blood pressure
SBP	systolic blood pressure
DBP	diastolic blood pressure
MAP	mean arterial pressure
RPP	rate pressure product
$\dot{V}O_2max$	maximal oxygen consumption
$M\dot{V}O_2$	myocardial oxygen consumption
GSH	glutathione
GSSG	oxidized glutathione
OSI	oxidative stress index
ROS	reactive oxygen species
LC3	microtubule-associated protein light chain 3
Atg7	autophagy related gene 7
TUNEL	terminal deoxynucleotidyl transferase dUTP nick end labelin
n	numbers

permeability, resulting in the loss of cell membrane integrity and function. Apoptosis is also a major pathway of myocardial cell loss after cardiac remodeling.[5,6] Inadequate adenosine triphosphate (ATP) generation and disrupted ion homeostasis in mitochondria contribute to the opening of mitochondrial transition pores, and lead to the release of cytochrome *c* into the cytoplasm, which activates caspase 3-mediated apoptosis.[7] Autophagy, a cellular process involved in the self-degradation and recycling of damaged cellular components, has been reported to occur in CMs following cardiac remodeling.[8] Autophagy is believed to play a cardioprotective role against cardiac remodeling.[8,9] Autophagy can either enhance survival or accelerate CMs death. However, autophagy can have a dual role in the responses of CMs to pathological conditions. It may represent a beneficial adaptive response to stress but can also lead to maladaptive responses linked to disease pathogenesis and cell-death induction.[10] While several studies support the notion that enhanced autophagy is cardioprotective, there are also reports that increased autophagy is detrimental to the heart.[11] Previous studies have demonstrated that exercise training can enhance autophagy in skeletal muscle, maintain its normal physiological activities, inhibit apoptosis caused by myocardial infarction (MI), decrease myocardial cell damage, and improve cardiovascular function.[12,13] Endurance exercise has been shown to protect against MI, with the effectiveness depending on the combination of exercise intensity, duration, frequency, and type.[14] Research conducted in the early 2000s indicated that exercise below approximately 50% of the maximal oxygen consumption ($\dot{V}O_2max$) does not provide protection against experimental MI in isolated perfused rodent hearts.[15] However, a study by Lennon et al. demonstrated that both moderate-intensity exercise (60 minute [min]/day at around 55% $\dot{V}O_2max$) and high-intensity treadmill exercise (60 min/day at approximately 75% $\dot{V}O_2max$) were equally effective in protecting against ischemia-reperfusion (IR) injury, suggesting cardioprotective benefits from both moderate and vigorous intensities.[16] Quindry et al. also reported the protective function of endurance training (70% $\dot{V}O_2max$) in dealing with oxidative stress, infarct sizes, and myocardial apoptosis in rats after ischemia-reperfusion injury.[17]

Another study conducted on rats found that the reduction in infarct size was proportional to the intensity of exercise. Specifically, rats trained at 60% $\dot{V}O_2max$ showed a smaller infarct size compared to those trained at 80% $\dot{V}O_2max$ over a period of 10 weeks.[18] Furthermore, the efficacy of exercise preconditioning (EP) in mitigating heart injury was improved as the EP intensity increased from 53.0% $\dot{V}O_2max$ to 74.0% $\dot{V}O_2max$. The effect was most pronounced when EP intensity was 74.0% $\dot{V}O_2max$, compared to all other setting EP groups.[19] The results suggest that high-intensity exercise may provide greater cardioprotective benefits, possibly due to the increase in aerobic fitness.[20]

EP is a concept similar to ischemic preconditioning (IP) that was introduced as a method to protect cardiac tissue.[15,21] Additionally, Meng et al. confirmed that EP decreases cardiac cell apoptosis, and long-term EP has more pronounced protective effects than short-term EP.[22] EP has been established to improves myocardial tolerance to I/R injury and provide significant cardioprotective effects against acute MI.[15,23] However, the underlying mechanisms of these cardioprotective effects are not yet fully understood. Aerobic interval training (AIT) is a non-invasive method that involves repeated bouts of relatively intense exercise interspersed with short periods of recovery through passive or moderate to low-intensity exercise.[24] AIT has recently gained attention and undergone extensive investigation as a hot topic for enhancing exercise performance in athletes.[25] AIT offers appropriate rest intervals, which are essential for maintaining exercise motivation and achieving training objectives. The controversy surrounding the intensity dependence of cardiac function underscores the importance of gaining a deeper understanding of how different treadmill running intensities can elicit a cardioprotective phenotype. Notably, research has revealed that exercising rats following a myocardial infarction can lead to the restoration of cardiac energy metabolism.[26]

The present study aimed to investigate the protective effects of two intensities of interval training against ISO-induced PCR in rats and to elucidate the underlying mechanisms behind these cardioprotective effects. The hypothesis was that different exercise loads would result in intensity-dependent cardioprotection. Therefore, the study examined whether MIIT and HIIT preconditioning could protect the myocardium by improving cardiac function and modulating the redox state in rats with ISO-induced PCR. Finally, the study aimed to explore the potential regulatory mechanisms involved and determine the optimal intensity capable of minimizing the effects of ISO on the myocardium.

2. Methods and materials

2.1. Animals ethical approval

In this study, thirty-eight healthy male Wistar rats (weighing 260 g–300 g and aged 8–10 weeks) were used. The animals were purchased from Animal House of Urmia University of Medical Sciences and were housed under standard conditions (temperature of [23 ± 2] °C, humidity of 50% ± 10% and a 12-hour [h] light/12-h dark cycle) with free access to water and food. All animal studies and experimental trials used conform to the Directive 2010/63/EU of the European Parliament and were approved and monitored by the ethical committee of laboratory animals, Urmia University (Approval NO: IR-UU-AEC-3/18).

Table 1
Exercise training protocol.

	Average maximum speed (meter/min)						HIIT			MIIT		
	Control ($n = 6$)	ISO ($n = 6$)	HIIT ($n = 4$)	HIIT + ISO ($n = 6$)	MIIT ($n = 4$)	MIIT + ISO ($n = 6$)	High intensity of interval training (85%–90% Smax)	Active recovery (50%–60% Smax)	Total running distance (m)	Moderate intensity of interval training (65%–70% Smax)	Active recovery (50%–60%Smax)	Total running distance (m)
pre	24.83 ± 0.47	24.00 ± 0.58	24.75 ± 0.63	24.00 ± 0.41	24.67 ± 0.33	23.20 ± 0.37						
Week1							19–20	11–12	1 010	13–14	11–12	770
Week2							20–21	12–13	1 070	14–15	12–13	830
Week3							21–22	13–14	1 130	15–16	13–14	890
Week4			29.50 ± 0.50	29.37 ± 0.42	26.50 ± 0.87	24.75 ± 0.59	23–24	14–15	1 230	16–17	14–15	950
Week5							24–25	15–16	1 290	17–18	15–16	1 010
Week6							25–26	16–17	1 350	18–19	16–17	1 070
Week7			35.25 ± 0.63	36.33 ± 0.49	31.25 ± 1.49	31.62 ± 0.90	27–28	17–18	1 450	20–21	17–18	1 170
Week8							28–29	19–20	1 530	21–22	18–19	1 230
Week9							30–31	20–21	1 630	22–23	19–20	1 290
Week10							30–31	20–21	1 630	22–23	19–20	1 290
Post	25.67 ± 0.80	16.67 ± 0.67 †	38.25 ± 1.65*	35.25 ± 2.84 #,$	35.33 ± 1.67*	22.20 ± 1.65 †						
***p* -values**		(† < 0.001)	(* < 0.001)	(# (0.001), $ (0.003)	(* (0.001)	(† (0.002)						

Results are expressed as the mean ± *SEM*. * as compared to the respective values of the sedentary control animals, # as compared to the respective values of the ISO-induced (ISO) animals and $ when compared MIIT + ISO with HIIT + ISO. Significance was determined by One-Way ANOVA followed by a Tukey Post-hoc test. † when ISO, MIIT + ISO, and HIIT + ISO compared to the control, MIIT, and HIIT respectively using an independent *t*-test. m:meter.

2.2. Experimental design and exercise protocols

The rats in the study were randomly divided into six groups: sedentary control (Control, $n = 6$), sedentary + ISO (ISO, $n = 8$), moderate-intensity interval training (MIIT, $n = 4$), moderate-intensity interval training + ISO (MIIT + ISO, $n = 8$), high-intensity interval training (HIIT, $n = 4$), and high-intensity interval training + ISO (HIIT + ISO, $n = 8$).

The sedentary control and ISO groups did not receive any exercise training and were only taken to the training room twice a week for 10 min of rest on the motionless treadmill. The MIIT and HIIT protocols were determined based on incremental load tests to establish the appropriate exercise intensity. The MIIT sessions consisted of 10 intervals of 4 min each at a higher load, performed at 65%–70% of the maximum running speed, interspersed with 2 min of active recovery at 50%–60% of the maximum running speed. Each MIIT session lasted for 60 min. The HIIT sessions also included 10 intervals of 4 min each at a higher load, but performed at 85%–90% of the maximum running speed, with 2 min of active recovery at 50%–60% of the maximum running speed. Each HIIT session also lasted for 60 min.[27] The running speeds for each session were determined based on the percentage of maximum running speed (Smax) and were adjusted to maintain relative exercise intensities throughout the 10-weeks training period, with 5 sessions per week (Table 1). The exercise sessions started with a 5 min warm-up and ended with a 5 min cool-down activity at 45% of the maximum running speed.[28] Electrical shocks were used only as motivation for the rats to run. Rats in the control and ISO groups did not undergo any additional exercise.

2.3. Pathological cardiac remodeling induction

For induction of cardiac remodeling, rats from the ISO, MIIT + ISO, and HIIT + ISO groups ($n = 8$ rats for each group) were subcutaneously administered with 100 mg/kg of ISO (Sigma-Alderich St. Luis, MO, USA) for two consecutive days with a 24 h interval. The ISO was dissolved in saline and injected based on body weight, following the model described by Soraya et al.[3] On the other hand, rats from the control group ($n = 6$), MIIT group ($n = 4$), and HIIT group ($n = 4$) received subcutaneous injections of a saline solution following the same schedule as the rats receiving ISO, serving as the control condition in the study. Unfortunately, two rats in ISO, MIIT + ISO, and HIIT + ISO groups died after the ISO injection.

2.4. Animal acclimatization to the treadmill

In the study, all animals underwent an acclimation process to the treadmill (Technic Azma, Model NT540, Tabriz, Iran) to minimize stress before beginning the exercise training protocols. The acclimation consisted of 5 training sessions, during which rats were placed on a stationary treadmill for 3 min without activating the shock grid. Subsequently, the treadmill was set to a walking speed of 6 m/min for 5 min and gradually increased to 12 m/min, resulting in a total exercise duration of 12 min.[29] For additional information and details, please refer to Table 2.

Table 2
Animal acclimation to the treadmill.

Stage	Speed (meter/min)	Elevation (% grade)	Duration (min)
1	0	0	3
2	6	0	5
3	9	0	2
4	12	0	2
			Total time: 12 min
			Total distance: 72 m

2.5. Exercise capacity test

Maximal exercise capacity was evaluated before and after the exercise training program, using a methodology similar to that by Li et al.[28] In order to monitor improvements in exercise performance and make adjustments running speed as necessary, an exercise capacity test was conducted. The test was performed 2 days following the adaptation period at the beginning of the training program, as well as at the end of the 3rd and 6th weeks, and at the end of the training protocol. During the exercise capacity test, rats started running on a treadmill at an initial speed of 8 m/min for 2 min. Subsequently, the speed was increased by 1 m/min every 2 min until the rats were no longer able to keep up with the treadmill speed and remained on the shockers for a continuous duration of over 10 seconds (s).[28] The results of the exercise capacity test are presented in Table 1.

2.6. Cardiac hemodynamic measurements

Blood pressure measurements were conducted using the PowerLab system, involving carotid artery cannulation. First, the pressure transducer was calibrated and filled with a heparinized physiological saline solution. The anesthetized animal was positioned in the supine position on the surgical table. A ventral midline incision was made on the neck, and the surrounding tissues, including the grafted tissues and adjacent muscles, were meticulously retracted to expose the left common carotid artery. The left common carotid artery was carefully isolated from the surrounding connective tissue, taking care not to stimulate the vagus nerve, which appears as a white structure. Fine forceps were used to separate the carotid artery from the vagus nerve. Two silk threads were passed beneath the artery, with one thread used to ligate the cephalic end and the other thread loosely tied approximately 1 cm from the upper tie to avoid blood pressure bifurcation. The cardiac end of the artery was temporarily clamped in preparation for cannulation. A small incision was made on the carotid artery using micro iris scissors, and a polyethylene cannula, pre-filled with heparinized normal saline, was carefully inserted into the blood vessel. Subsequently, hemodynamic parameters such as systolic blood pressure, diastolic blood pressure, mean arterial blood pressure, and heart rate were recorded and analyzed using LabChart 7 software.[3]

2.7. Tissue sampling and relative weighting

Following hemodynamic measurements, the hearts were rapidly excised and rinsed with cold saline to remove superficial connective tissue. The heart weight to body weight ratio (mg/g) was then employed to evaluate the degree of hypertrophy.[3]

2.8. Histopathological examinations

The apex of the cardiac tissues was fixed in a 10% formalin solution, then rinsed with water and dehydrated using graded alcohols. The tissues were then embedded in paraffin, and 5 μm sections were cut (3 samples for each group) using an automatic microtome (LKB, UK). Subsequently, the sections underwent Hematoxylin and Eosin (H&E) staining and were examined under light microscopy at × 400 magnification for morphometric analysis. Two independent examiners employed a morphological scoring system, assigning scores of 0, 1, 2, and 3 indicate the absence of detection, low, moderate, and intense pathological changes, respectively. The assessment of myocardial damage based on the H&E staining was determined as the average of the scores from the two examiners. Inflammatory cell infiltration, necrosis, hemorrhage, and edema were evaluated in the slides.

Table 3
Primers list details. Note: AT: annealing temperature; bp: base pair.

Gene	Primer	AT	bp
P62	F: GCTGCTCTCTTCAGGCTTACAG R: CCTGCTTCACAGTAGACGAAAG	53 °C	22
Beclin-1	F: AGCACGCCATGTATAGCAAAGA R: GGAAGAGGGAAAGGACAGCAT	51 °C	22
Atg7	F: AGCCTGTTCATCCAAAGTTCT R: CTGTGGTTGCTCAGACGGT	46 °C	21
LC3 I	F: GATGTCCGACTTATTCGAGAGC R: TTGAGCTGTAAGCGCCTTCTA	46 °C	22
GAPDH	F: AAGGTCATCCATGACAACTT R: GGCCATCCACAGTCTTCTGG	58 °C	20

2.9. Immunohistochemical staining and quantification of LC3-I/II and caspase-3 proteins

For immunohistochemical analysis, 4 μm sections were prepared to heating in a hot air oven at 60 °C for 25 min. Subsequently, the sections underwent deparaffinization and rehydration using graded alcohol concentrations. Antigen retrieval was performed using sodium citrate buffer (pH 7.2), followed by blocking endogenous peroxidases with 3% hydrogen peroxide for 5 min. To block nonspecific antigens, the slides were treated with a super blocker solution in PBS for 10 min. Following PBS washing, the slides were incubated overnight at 4 °C in a humidified chamber with primary antibodies (LC3I/II and caspase-3 at a dilution of 1:100). The secondary antibody used was peroxidase/HRP conjugated Goat Anti-Rabbit IgG, and the slides were incubated for 1 h at 37 °C. Diaminobenzidine (DAB) chromogen was used to stain the proteins, resulting in brown color, while hematoxylin was used to stain the nuclei. Negative control slides were prepared using normal IgG instead of the primary antibody. The stained slides were observed under a microscope. The quantification of LC3-I/II$^+$ and caspase-3$^+$ cells was performed by counting the positive cells per mm^2 of tissue in one section per group, and the percentages of positive cells were evaluated. To decrease the bios problem, the software analyzed the pixel-based intensities of brown reactions (representing targeted proteins) in 1 360 μm × 1 360 μm of tissue using image pro-insight software (Media Cybernetics, USA).

2.10. Evaluation of pro-oxidant-antioxidative balance in myocardial tissue

To assess the overall oxidation-antioxidation balance in myocardial tissue, commercially available kits were used to measure total antioxidant capacity (TAC) and total oxidant status (TOS) (Navand Salamat Co., Iran). A 20 mg sample of cardiac tissue was homogenized in 1 000 μl of lysis buffer. After centrifugation (10 000 rpm) for 10 min at 4 °C, the clear supernatant was collected and stored at −20 °C for further biochemical analysis.

To assess myocardial TAC, a reaction was conducted in a 1 000 μl reaction buffer comprising 100 μl supernatant, 400 μl distilled water, and 500 μl ABTS$^+$ buffer. The absorbance at 492 nm was measured after 5 min of incubation at room temperature. TAC levels were calculated using a formula derived from standards' optical densities (ODs) and concentrations, and the results were expressed as nmol/mg protein. To measure myocardial TOS, a reaction buffer was prepared using 20 μl of the sample, 133.5 μl of reaction buffer 1, and 6.5 μl of reaction buffer 2 provided by the kit. The mixture was incubated for 10 min at room temperature, and the absorbance was measured at a wavelength of 530 nm using an enzyme-linked immunosorbent assay (ELISA). TOS levels were calculated using a formula derived from standards' ODs and concentrations, and the results were expressed as μmol Equiv./L. Finally, the oxidative stress index (OSI) was calculated as the ratio of the TOS level to the TAC level.

The GSH and GSSG levels in cardiac tissues were measured using the GSSG/GSH quantification kit (Dojindo Molecular Technologies Inc., Kumamoto, Japan). For quantification, 50 mg tissue were homogenized with 1 mL of 5% (v/v) 5-sulfosalicylic acid. The resulting mixture was centrifuged at 8 000 × *g* for 10 min at 4 °C. The levels of total GSH and

oxidized GSH (GSSG) in the supernatant were determined according to the manufacturer's protocol. The GSH levels were calculated using the following formula: GSH (μmol/L) = total GSH (μmol/L) − 2 × GSSG (μmol/L), where the concentrations of total GSH and GSSG were used. The amounts of GSH and GSSG were determined by referencing a standard curve.

2.11. TUNEL staining

The cardiac tissues were sectioned into 4 μm slices and fixed in acetone at room temperature for 24 h. The samples were then transferred to a solution containing terminal deoxynucleotidyl transferase and detection buffer (Roche Diagnostics GmbH), conjugated with horseradish peroxidase, and incubated at 37 °C for 60 min. A diaminobenzidine chromogen (Boehringer) was used for visualization. To determine the number of TUNEL-positive nuclei, several additional steps were undertaken. The samples were examined using a light microscope (CKX53; Olympus Corporation) at × 400 magnification. A random area was selected, and the nuclei within that area were counted. The resulting value was converted to a percentage by dividing it by the total number of cell nuclei. To decrease the bios problem, the pixel-based intensities of brown reactions (representing apoptotic cells) were analyzed in 1 180 μm × 1 180 μm of tissue using image pro-insight software (Media Cybernetics, USA).

2.12. mRNA extraction, cDNA synthesis, and qRT-PCR

The mRNA expressions of Beclin-1, Atg-7, p62, and LC3-I were measured using RT-qPCR. Total RNA was extracted from 0.2 g myocardial tissues (n = 4–6 from each group) using TRIzol reagent (Takara, Japan). The RNA concentration and purity were measured using a NanoDrop-1000 spectrophotometer (Thermo Scientific, Washington, USA), and only samples with A260/A280 values between 1.8 and 2.0 were utilized. The RNA samples were stored at −20 °C.

For cDNA synthesis, 1 μg of total RNA from each sample was used with the Takara PrimeScript RT reagent kit. The resulting cDNA served as a template for PCR amplification using specific forward and reverse primers (Table 3). qPCR was performed in 10 μL reactions, consisting of 5 μL of 2 × PowerUp SYBR Green Master Mix (Thermo Fisher Scientific), 2 μL of cDNA template, 0.3 μL of each primer (10 nM forward and reverse primers), and water. The reaction was carried out in a BioRad CFX ConnectTM Optics Module (BioRad, Hercules, CA, USA) with the following cycling conditions: predenaturation at 95 °C for 5 min, 40 cycles of 95 °C for 30 s, and 60 °C for 1 min, and a melting curve analysis from 60 °C to 95 °C. Real-time fluorescence values were recorded and used to determine the threshold cycle (CT). Gene expression analysis was performed as follows: the CT value of each target gene was normalized to the CT value of each target gene (GAPDH), and the $2^{(-\Delta\Delta CT)}$ method was employed to calculate the expression of each target gene.

2.13. Statistical analysis

The data were presented as mean ± standard error of the mean (*SEM*). The normality of the distribution for all variables was assessed using the Kolmogorov-Smirnov test, and the homogeneity of variances was evaluated using Levene's test. One-way ANOVA was conducted to determine the effects of EP on the studied variables, followed by Tukey's HSD post-hoc analyses. An independent t-test was performed to compare the two groups. Data analysis was conducted using IBM SPSS Statistics version 26 (IBM Corp., Armonk, NY, USA), and GraphPad Prism 8 software was utilized for drawing diagrams. The significance level was set at $p \leq 0.05$.

3. Results

3.1. Effects of MIIT and HIIT exercises on relative heart weight and cardiac hypertrophy

The results showed that the relative heart weight to body weight was not significantly affected by the MIIT and HIIT exercises in their respective groups when compared to the ISO rats. The mean heart weight in the ISO group (54.56%) was significantly increased compared to the control rats. The HIIT + ISO group showed a reduction in heart weight compared to the ISO rats ($p = 0.021$). There was no significant change in the heart weight of the MIIT + ISO group compared to the ISO induce rats. In terms of the relative heart weight to total body weight, the ISO (55.69%), MIIT + ISO (54.96%), and HIIT + ISO (40.68%) groups exhibited a significant increase compared to the control group. This increase was not due to a decrease in body weight but mainly attributed to an increase in heart weight, indicating cardiac hypertrophy (Table 4).

3.2. Exercise tolerance and functional capacity

Before the initiation of the exercise protocol, there were no significant differences in maximum running speed among various groups. Following the experimental period, both the HIIT and MIIT groups demonstrated higher functional capacity in comparison to the control group. Notably, the HIIT + ISO group exhibited the highest functional capacity, surpassing both the ISO and MIIT + ISO groups. The maximum running speeds were recorded as follows: control ([25.67 ± 0.80] m/min), ISO ([16.67 ± 0.67] m/min), MIIT ([35.33 ± 1.67] m/min), HIIT ([38.25 ± 1.65] m/min), MIIT + ISO ([22.20 ± 1.65] m/min), and HIIT + ISO ([35.25 ± 2.84] m/min) (refer to Table 1). This suggest that the maximum running speeds were not diminished following ISO induction in comparison to HIIT group. However, a decrease was observed in the MIIT + ISO group.

3.3. Histopathological findings

The H&E staining was performed to validate the ISO induced PCR and

Table 4
Body weight, heart weight, heart weight to body weight ratio for the different groups.

Groups	Control (n = 6)	ISO (n = 6)	MIIT (n = 4)	MIIT + ISO (n = 6)	HIIT (n = 4)	HIIT + ISO (n = 6)	p-values
Initial body weight (g)	275.17 ± 6.09	277.50 ± 5.12	275.00 ± 6.34	274.13 ± 5.44	275.50 ± 4.66	280.25 ± 4.55	Non-sig.
Final body weight (g)	375.80 ± 12.22	371.40 ± 6.07	349.33 ± 4.98	356.40 ± 10.77	365.00 ± 8.26	337.80 ± 8.49	Non-sig.
Heart weight (mg)	920.00 ± 23.45	1 422.00 ± 17.15 †	913.33 ± 6.67	1 440.00 ± 36.06 †	957.50 ± 17.02	1 250.00 ± 62.61 #, $, †	(# 0.021, $ 0.009, † < 0.001)
Heart weight/Body weight (mg/g)	2.46 ± 0.09	3.83 ± 0.10 †	2.62 ± 0.02	4.06 ± 0.18 †	2.63 ± 0.04	3.70 ± 0.18 †	† (< 0.001)

Results are expressed as the mean ± *SEM*. # as compared to the respective values of the ISO-induced (ISO) animals and $ when compared MIIT + ISO with HIIT + ISO (Significance was determined by One-Way ANOVA followed by a Tukey Post-hoc test). † when ISO, MIIT + ISO, and HIIT + ISO compared to the control, MIIT, and HIIT respectively using an independent t-test.

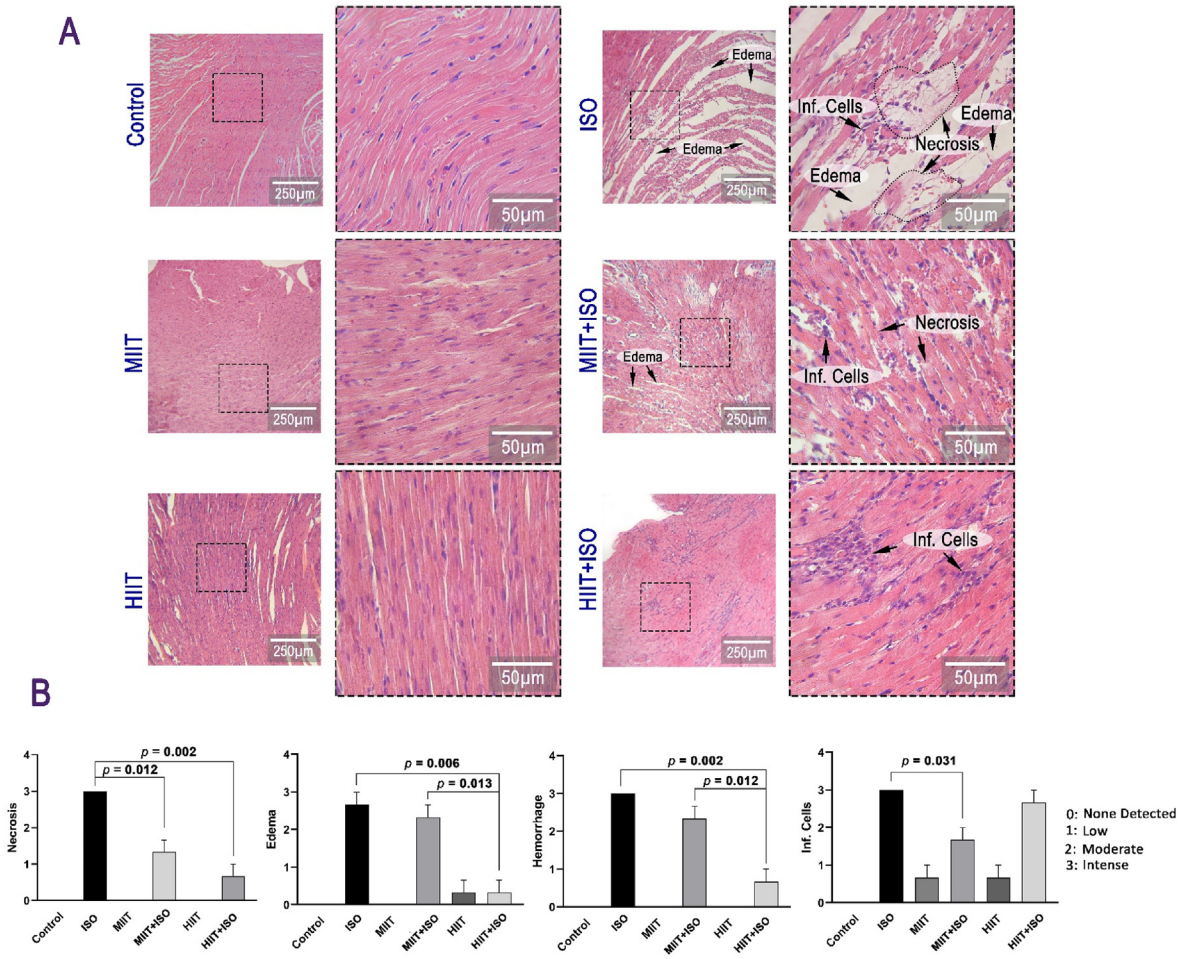

Fig. 1. Effects of exercise preconditioning on cardiac histological changes under a light microscope (H&E [x 400]). (A) The cardiac section of control, MIIT, and HIIT rats show normal cardiac architecture with a proper myofibrillar arrangement without any abnormal histopathological changes. While the cardiac section of ISO-induced PCR rats (ISO) depict disoriented myofibril with intense infiltration of inflammatory cells, interstitial edema many necrotic changes, and disruption of cardiac myofibrils (arrow mark). The cardiac section of rats preconditioned with exercise before ISO-induced PCR (MIIT + ISO and HIIT + ISO) display mild infiltrations of inflammatory cells and mild degenerative changes of myocardial tissue. (B) Histological injury scores of the myocardial tissue. Sedentary control (control), (ISO)-induced pathological cardiac remodeling (ISO), moderate intensity of aerobic interval training (MIIT), high intensity of aerobic interval training (HIIT), moderate intensity of aerobic interval training + ISO (MIIT + ISO) and high intensity of aerobic interval training + ISO (HIIT + ISO). Results are expressed as the mean ± *SEM* (n = 3 rats for each group). Significance was determined by One-Way ANOVA followed by a Tukey Post-hoc test.

Table 5
Parameters of Hemodynamic and electrocardiogram data values.

Groups	Control (n = 6)	ISO (n = 6)	MIIT (n = 4)	MIIT + ISO (n = 6)	HIIT (n = 4)	HIIT + ISO (n = 6)
Arterial blood pressure (mmHg)	148.60 ± 6.06	128.20 ± 2.80 †	185.67 ± 0.88 *	156.00 ± 3.78 $^{\#,\dagger}$	149.25 ± 5.81 $^{\&}$	143.40 ± 5.94
Systolic Blood Pressure (mmHg)	150.00 ± 5.54	129.20 ± 2.29 †	186.67 ± 1.20 *	156.60 ± 3.66 $^{\#,\dagger}$	151.25 ± 2.14 $^{\&}$	144.60 ± 5.90
Diastolic Blood Pressure (mmHg)	125.40 ± 1.81	111.20 ± 3.48 †	146.33 ± 1.45 *	135.20 ± 2.58 $^{\#,\dagger}$	128.75 ± 1.75 $^{\&}$	122.40 ± 3.22 $^{\$}$
Mean arterial pressure (mmHg)	133.20 ± 2.96	116.60 ± 2.25 †	159.00 ± 1.15 *	142.00 ± 2.79 $^{\#,\dagger}$	135.75 ± 1.65 $^{\&}$	129.20 ± 3.72 $^{\#,\$}$
RPP	349.83 ± 14.92	422.53 ± 26.68 †	435.47 ± 6.12 *	540.95 ± 49.32	374.43 ± 11.61 $^{\&}$	377.21 ± 7.17 $^{\$}$
$M\dot{V}O_2$ (ml·100g LV·min^{-1})	42.68 ± 2.09	52.85 ± 3.73 †	54.67 ± 0.86 *	69.43 ± 6.90	46.12 ± 1.63 &	46.51 ± 1.00 $
Heart rate (bpm)	233.20 ± 4.84	326.40 ± 16.91 †	233.33 ± 4.41	344.20 ± 26.87 †	247.50 ± 6.20	262.60 ± 12.09 $^{\$}$

Results are expressed as the mean ± *SEM*: myocardial oxygen consumption, $M\dot{V}O_2$ (ml· 100 g LV· min^{-1}) = 0.14 (HR × SBP × 0.01) - 6.3. RPP, rate pressure product, RPP (no units) = HR (beats·min^{-1}) × SBP (mmHg) × 0.01. MAP, mean arterial pressure, MAP (mmHg) = DBP (mmHg) + 0.32 (pulse pressure; i.e., SBP, systolic blood pressure – DBP, diastolic blood pressure). * as compared to the respective values of the sedentary control animals, $^{\#}$ as compared to the respective values of the ISO-induced (ISO) animals, $^{\&}$ when compared MIIT with HIIT and $^{\$}$ when compared MIIT + ISO with HIIT + ISO (Significance was determined by One-Way ANOVA followed by a Tukey Post-hoc test). † when ISO, MIIT + ISO, and HIIT + ISO compared to the control, MIIT, and HIIT respectively using an independent t-test. $^{*,\#,\&,\$,\dagger}$ $p \leq 0.05$.

the protective effects of exercise preconditioning. In the control group, CMs exhibited an orderly arrangement with no observable histopathological changes. In contrast, the ISO-induced PCR group showed broken myocardial fibers, significant edema, hemorrhage, and a noticeable infiltration of inflammatory cells. Interestingly, these pathological changes were effectively alleviated in the MIIT + ISO and HIIT + ISO groups, indicating a protective effect of exercise preconditioning on ISO-induced PCR (Fig. 1A and B). Consequently, significantly lower immune cell infiltration, controlled edema, and lower alteration in the myocardial histological structure, and no hemorrhage were observed in the MIIT + ISO and HIIT + ISO groups. A comparative analysis between the MIIT and HIIT exercise protocols revealed that HIIT provided a superior level of

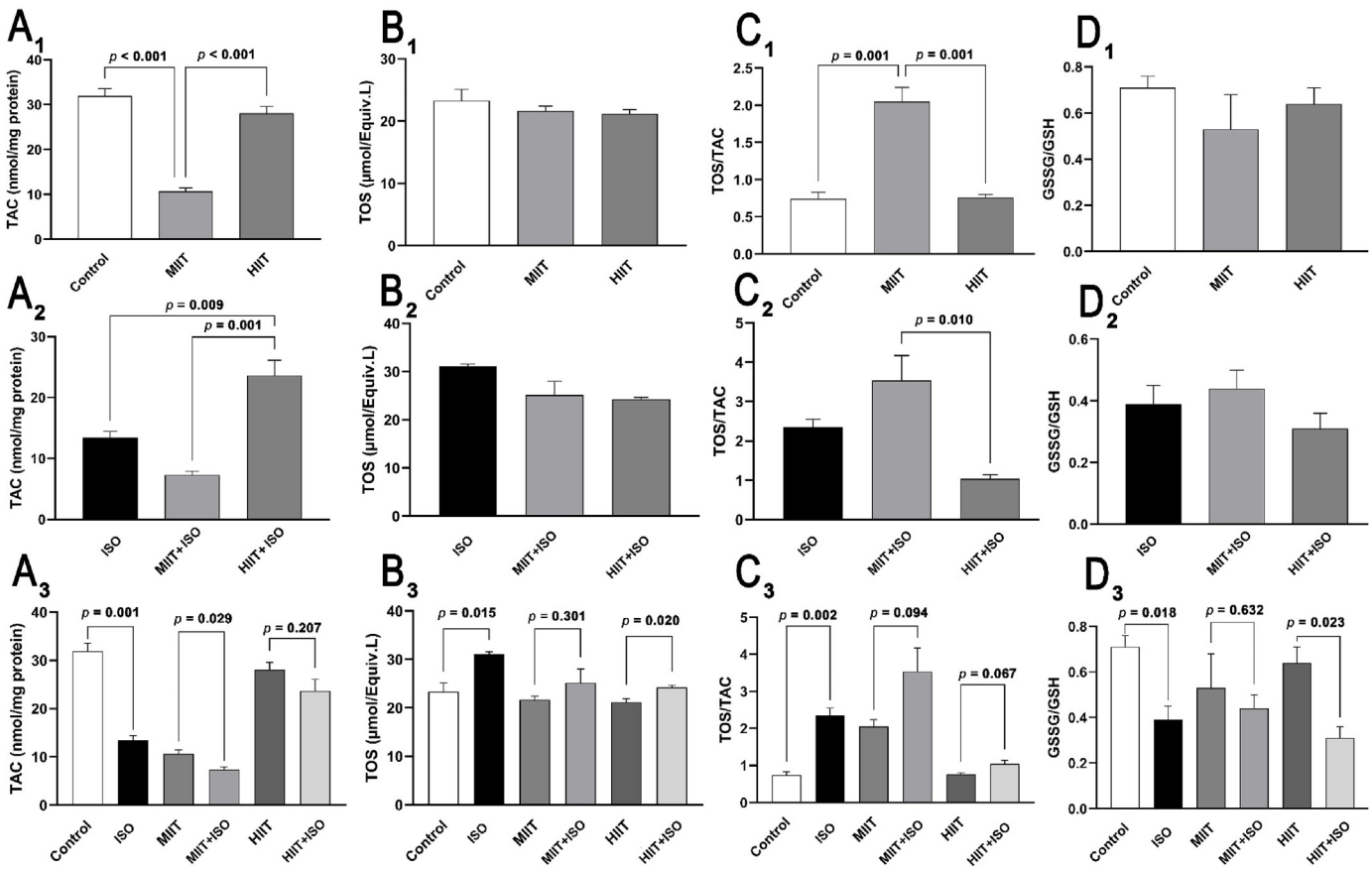

Fig. 2. Mean changes in the myocardial. ($A_{1,2,3}$) Total antioxidant capacity (TAC), ($B_{1,2,3}$) total oxidant status (TOS), ($C_{1,2,3}$) oxidative stress index (OSI, TOS to TAC ratio), and ($D_{1,2,3}$) the relative ratio of the oxidized glutathione to glutathione (GSSG/GSH). Sedentary control (control, $n = 6$), (ISO)-induced pathological cardiac remodeling (ISO, $n = 6$), moderate intensity of aerobic interval training (MIIT, $n = 4$), high intensity of aerobic interval training (HIIT, $n = 4$), moderate intensity of aerobic interval training + ISO (MIIT + ISO, $n = 6$) and high intensity of aerobic interval training + ISO (HIIT + ISO, $n = 6$). Results are expressed as the mean ± *SEM*. Significance was determined by One-Way ANOVA followed by a Tukey Post-hoc test ($A_{1,2}$, $B_{1,2}$, $C_{1,2}$, $D_{1,2}$). Data were analyzed using the Student's *t*-test (A_3, B_3, C_3, D_3).

protection to the CMs when compared to the MIIT group.

3.4. Effects of MIIT and HIIT exercises on ISO-induced cardiac dysfunction in rats

The evaluation of hemodynamic parameters revealed that the ISO group exhibited an increase in HR, rate-pressure product, and myocardial oxygen consumption ($M\dot{V}O_2$). In contrast, there was a decrease in arterial blood pressure (ABP), systolic blood pressure (SBP), diastolic blood pressure (DBP), and mean arterial pressure (MAP) when compared to the control group. However, the HIIT preconditioning programs demonstrated a significant improvement in ISO-induced cardiac dysfunction. Specifically, the HIIT preconditioning programs (as seen in the HIIT + ISO group) effectively preserved the progressively declining levels of ABP, SBP, DBP, MAP, HR, rate-pressure product, and $M\dot{V}O_2$ induced by ISO, as depicted in Table 5.

3.5. Effects of MIIT and HIIT exercises on pro-oxidant-antioxidant balance in cardiac tissue

The study aimed to investigate the effects of AIT preconditioning on the pro-oxidant-antioxidant balance in the heart following ISO induction. To achieve this, the total antioxidant capacity (TAC), total oxidant status (TOS), and the TOS to TAC ratio were assessed and compared among the experimental groups. The ISO group exhibited a significant decrease in TAC levels and an elevation in TOS levels when compared to the control group (Fig. 2 A_3, B_3). In contrast, HIIT demonstrated higher efficacy in lowering TOS levels and restoring the TOS/TAC balance in the cardiac tissue. No statistically significant differences in TOS levels alone were observed between the MIIT, HIIT, and control groups (Fig. 2). Furthermore, the ISO group showed a significant change in the mean relative GSSG/GSH level compared to the control group (Fig. 2 D_3).

3.6. Effects of MIIT and HIIT exercises on autophagy markers

The study aimed to investigate the impact of preconditioning AIT at different intensities on autophagy in ISO-induced PCR conditions. The mRNA levels of key autophagy-related genes, including Beclin-1, Atg-7, LC3, and p62 were assessed to autophagic activity (Fig. 3A, B, 3C, 3D). The ISO group exhibited a significant increase in the mRNA levels of Atg-7 ($p = 0.001$), Beclin-1, LC3, and p62 ($p < 0.001$) compared to the control group (Fig. 3 A_3, B_3, C_3, D_3). However, the application of variable intensity AIT resulted in a significant down-regulation of the mRNA expressions of Beclin-1, Atg-7, LC3, and p62 compared to the ISO group. To further explore the effect of AIT preconditioning on autophagy and phosphorylated LC3 (activated form), immunostaining for LC3I/II was performed. The ISO group demonstrated a significant ($p = 0.005$) increase in the immunoreactivity of LC3I/II compared to the control group. Similarly, both the MIIT and HIIT groups showed significantly higher percentages of $LC3I/II^+$ cells per mm^2 of tissue compared to the control rats. Additionally, the MIIT + ISO group exhibited a decreased number of $LC3I/II^+$ cells compared to the ISO group, while the HIIT + ISO group showed a significantly higher number of $LC3I/II^+$ cells compared to the ISO group. Moreover, the MIIT + ISO group demonstrated a lower

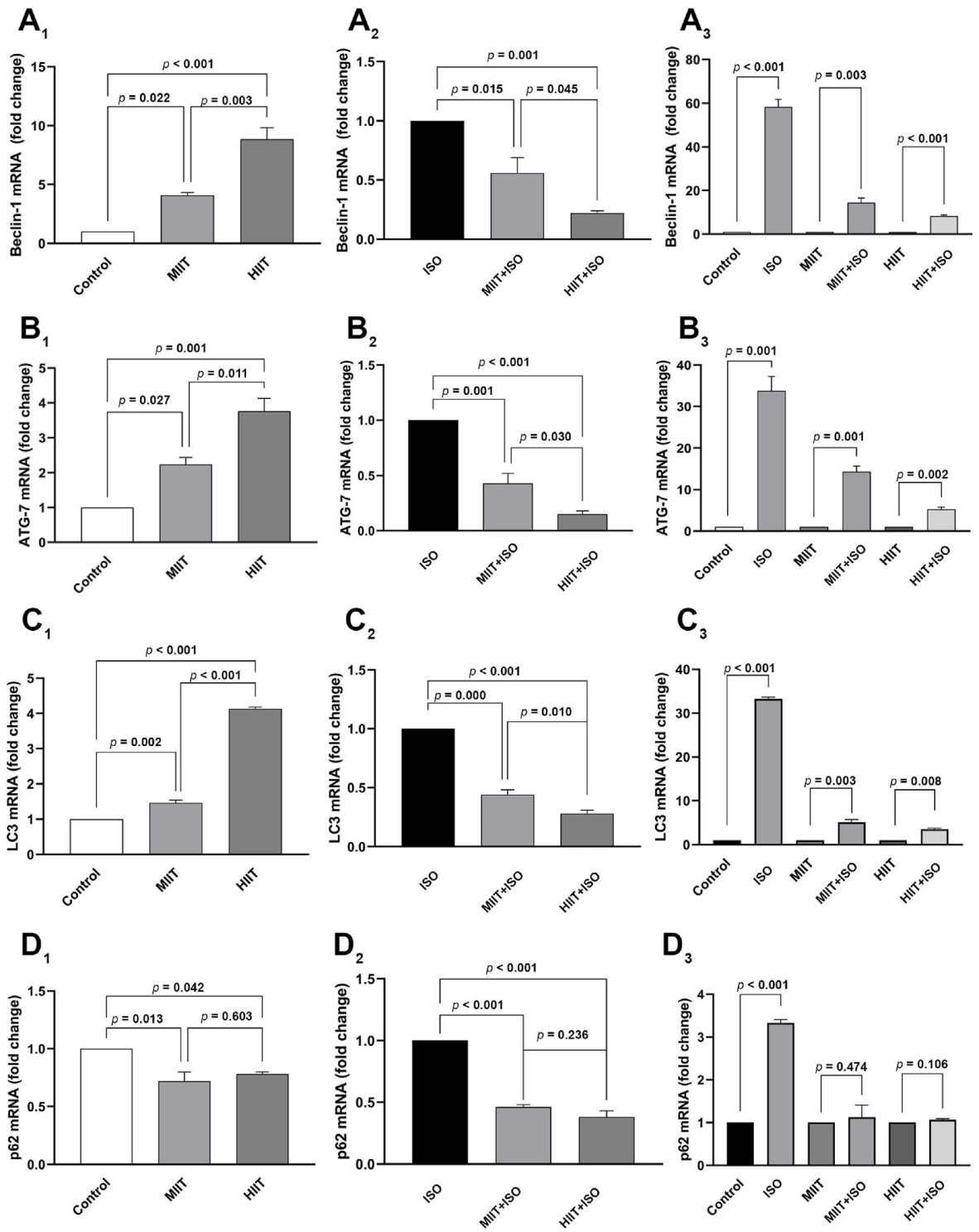

Fig. 3. The mRNA expression levels detected by RT-qPCR. Relative mRNA expressions of ($A_{1,2,3}$) Becline-1, ($B_{1,2,3}$) Atg-7, ($C_{1,2,3}$) LC3, and ($D_{1,2,3}$) p62 in cardiac tissues of rats with sedentary control (control, $n = 6$), (ISO)-induced pathological cardiac remodeling (ISO, $n = 6$), moderate intensity of aerobic interval training (MIIT, $n = 4$), high intensity of aerobic interval training (HIIT, $n = 4$), moderate intensity of aerobic interval training + ISO (MIIT + ISO, $n = 6$) and high intensity of aerobic interval training + ISO (HIIT + ISO, $n = 6$). Significance was determined by One-Way ANOVA followed by a Tukey Post-hoc test ($A_{1,2}$, $B_{1,2}$, $C_{1,2}$, $D_{1,2}$). Data were analyzed using the Student's *t*-test (A_3, B_3, C_3, D_3). All data are expressed as mean ± *SEM*.

percentage of LC3I/II^{+} cells compared to the ISO group, whereas the HIIT + ISO group exhibited a higher percentage of LC3I/II^{+} cells compared to the ISO group (Fig. 4A, B, 4C).

3.7. Effects of MIIT and HIIT on active caspase-3 expression

The IHC staining results revealed a significant ($p = 0.001$) increase in the average percentage of caspase-3^{+} cells *per* mm^2 of tissue in the ISO group compared to the control rats (Fig. 5A, B, 5C). Conversely, this trend was reversed in the MIIT + ISO and HIIT + ISO groups, which showed significantly lower levels of caspase-3^{+} cells compared to the ISO group.

3.8. Effects of MIIT and HIIT exercises on apoptosis

The study aimed to evaluate the pro-apoptotic effect of ISO and the protective effects of AIT using TUNEL staining. The analysis revealed a significant increase in the percentage of TUNEL-positive cells (per one mm^2 of tissue) in the ISO group (80.05% ± 3.87%) compared to the control animals (Fig. 6 C_3). However, both the MIIT and HIIT groups under ISO-induced conditions (MIIT + ISO and HIIT + ISO) demonstrated a decrease in the percentages of apoptotic cells per one mm^2 of tissue (Fig. 6A, B, 6C).

4. Discussion

Numerous factors are implicated in the initiation and progression of cardiac remodeling in response to pathological stressors. Despite advancements in clinical interventions, cardiac remodeling continues to be a primary contributor to mortality rates. Pathophysiological and morphological changes induced by ISO in the cardiac tissues of experimental animals have been reported to bear resemblance to those observed in the myocardial tissues of humans post-infarction.[1] The process of ISO-induced cardiac remodeling encompasses injury, necrosis, apoptosis of cardiac cells, and disruption of energy reserves in CMs, culminating in cardiac dysfunction. The condition is marked by substantial damage to CMs. A variety of exercise training protocols, in conjunction with certain medications, are advocated to achieve therapeutic goals. Post-MI exercise training has been empirically shown to

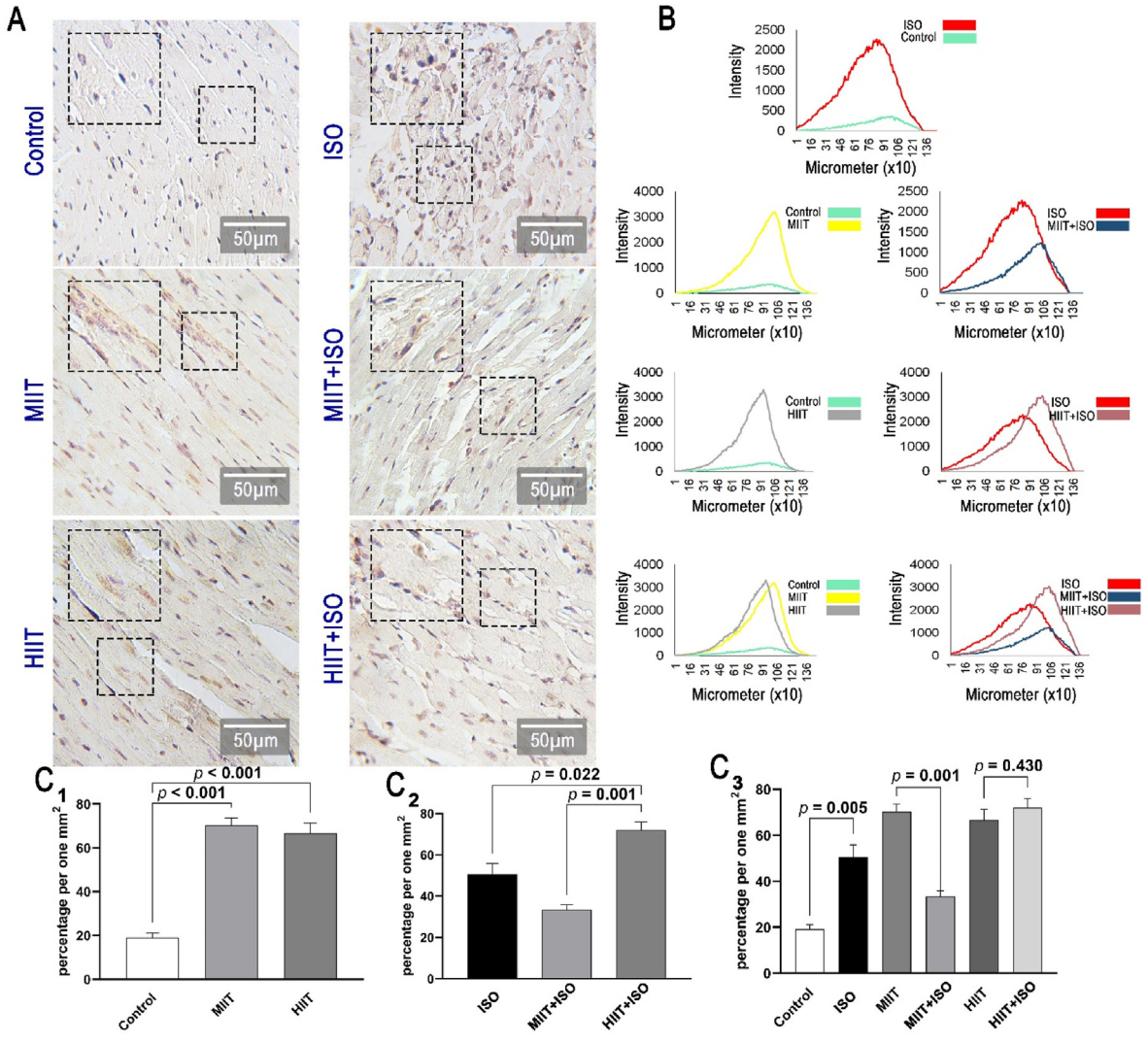

Fig. 4. (A) Effect of exercise preconditioning on autophagy-related protein expressions by immunohistochemistry ($n = 3$ rats for each group). Representative photographs of myocardial tissues with immunohistochemistry staining of LC3I/II. (B) Software analysis for pixel-based intensity for brown reactions (representing positive reaction for LC3I/II) in different sections from different groups in 1 360 μm × 1 360 μm of tissue. ($C_{1,2,3}$) Mean changes in the percentages of LC3 I/II^{+} cells/one mm^2 of tissue in different groups. Sedentary control (control), (ISO)-induced pathological cardiac remodeling (ISO), moderate intensity of aerobic interval training (MIIT), high intensity of aerobic interval training (HIIT), moderate intensity of aerobic interval training + ISO (MIIT + ISO) and high intensity of aerobic interval training + ISO (HIIT + ISO). Significance was determined by One-Way ANOVA followed by a Tukey Post-hoc test ($C_{1,2}$). Data were analyzed using the Student's *t*-test (C_3). All data are presented as mean ± *SEM*.

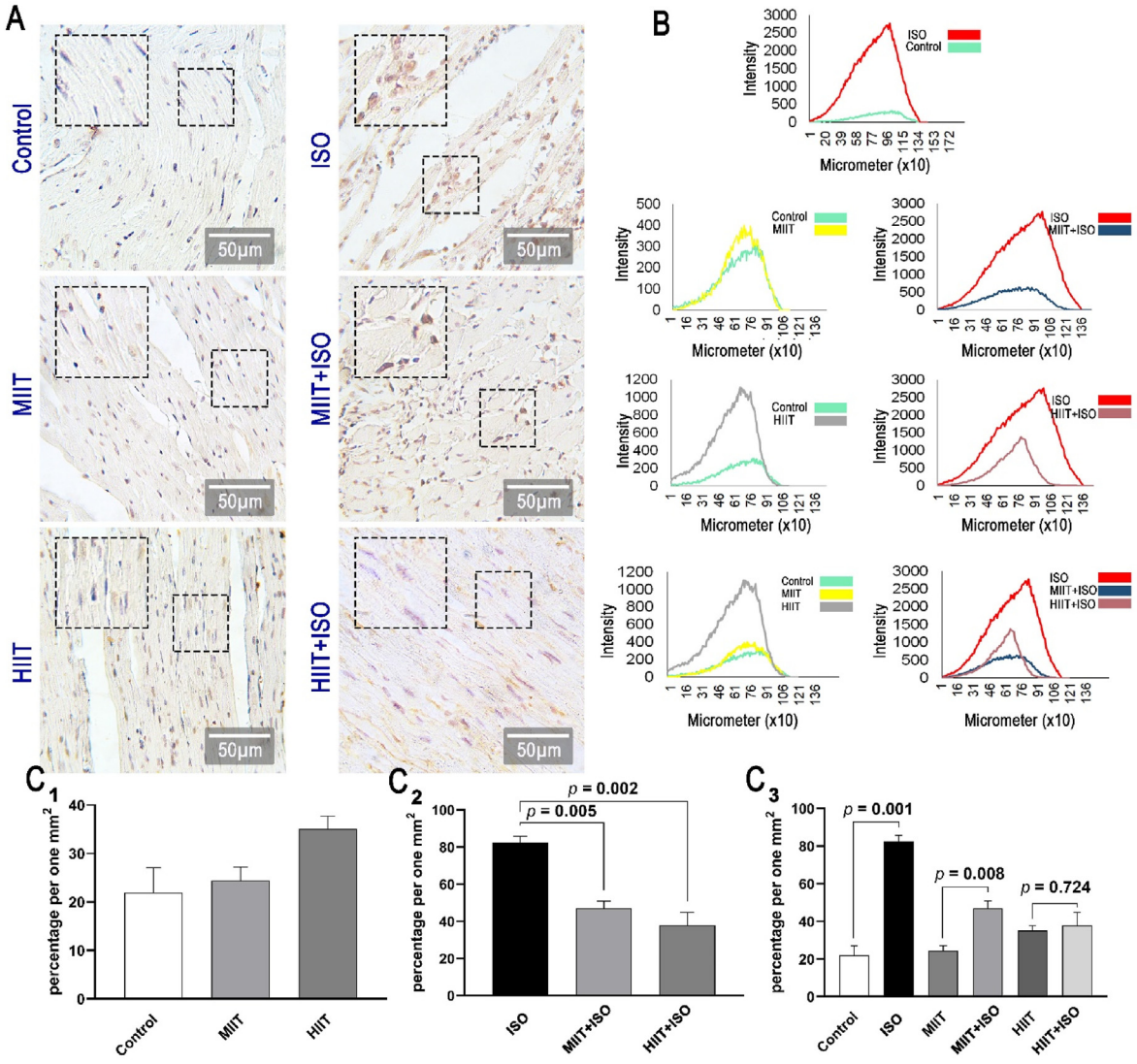

Fig. 5. (A) Effect of exercise preconditioning on caspase-3 protein expressions by immunohistochemistry (n = 3 rats/each group). Representative photographs of myocardial tissues with immunohistochemistry staining of caspase-3. (B) Software analysis for pixel-based intensity for brown reactions (representing positive reaction for caspase-3) in different sections from different groups in 1 360 μm × 1 360 μm of tissue. ($C_{1,2,3}$) Mean changes in the percentages of caspase-3 positive cells/one mm^2 of tissue in different groups. Sedentary control (control), (ISO)-induced pathological cardiac remodeling (ISO), moderate intensity of aerobic interval training (MIIT), high intensity of aerobic interval training (HIIT), moderate intensity of aerobic interval training + ISO (MIIT + ISO) and high intensity of aerobic interval training + ISO (HIIT + ISO). Significance was determined by One-Way ANOVA followed by a Tukey Post-hoc test ($C_{1,2}$). Data were analyzed using the Student's *t*-test (C_3). All data are presented as mean ± *SEM*.

improve metabolic equivalents (METs), enhance circulatory function, and decrease the risk of chronic diseases and overall mortality.[30,31] Consistent with these findings, additional studies have suggested that moderate interval exercises can accelerate the cardiopulmonary rehabilitation process and the remodeling of the left ventricle (LV) in patients experiencing LV dysfunction post-MI.[32,33] This underscores the potential benefits of exercise as a non-pharmacological intervention in the management of cardiac conditions. Interestingly, Quindry et al. have shown that short-term EP with 70% $\dot{V}O_2$max has a preventive effect on heart ischemia-reperfusion injury including improved myocardial antioxidant capacity and prevention of caspase-3 activation.[34]

Hence, the ameliorative impact of exercise training protocols has been acknowledged as adjuvant treatments in conjunction with various medications, albeit depending on their intensity and duration.[35] However, the persisting query is how AIT preconditioning can mitigate the adverse effects of ISO, thereby protecting the myocardium from pathological remodeling. Therefore, the present study examined whether AIT preconditioning exhibited protective effect on ISO-induced detrimental effects by revealing any alterations in the heart oxidant/antioxidant balance, its relationship to autophagy initiation and progression, and finally the possibility of controlling apoptosis following ISO induction in rats.

As previously mentioned, various training protocols have been demonstrated to enhance cardiac functionality following PCR. To evaluate their protective effects, rather than supportive ones on PCR, we examined any alterations in ABP, SBP, DBP, MAP, HR, RPP, and the $M\dot{V}O_2$ ratio before and after ISO induction in MIIT and HIIT groups. The present study revealed that ISO-induced PCR increased HR, RPP, and $M\dot{V}O_2$ and significantly decreased ABP, SBP, DBP, and MAP compared to sedentary control rats indicating severe cardiac dysfunction. Furthermore, we observed a significant increase in heart weight in ISO group along with changes in cardiac weight relative to total body weight, representing another phenotype for PCR. Indeed, it has been demonstrated that an increase in heart rate is responsible for increased oxygen consumption, leading to accelerated myocardial necrosis.[36] Next, a pathological analysis was conducted to confirm that ISO induced PCR

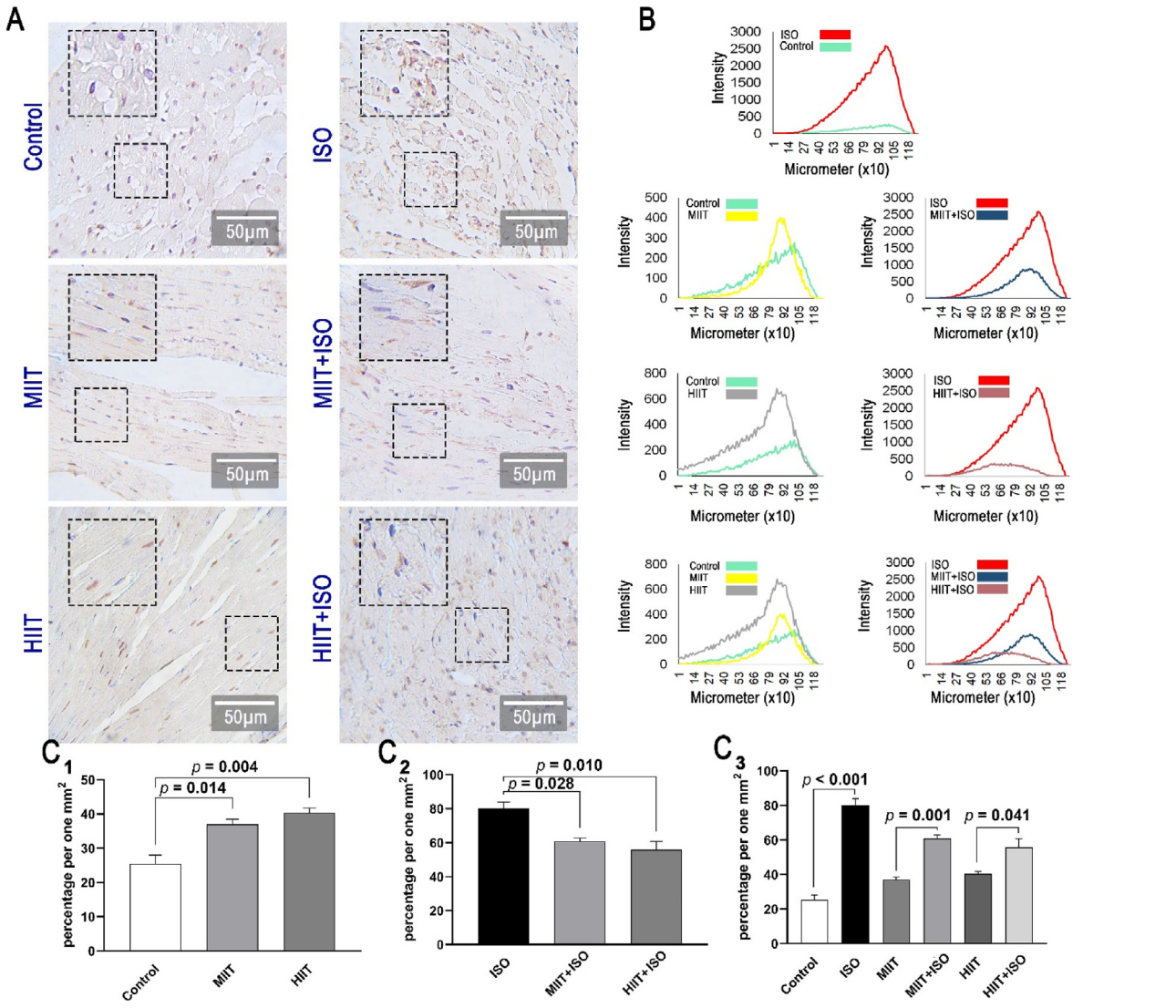

Fig. 6. Analysis of cardiomyocyte apoptotic index. Exercise preconditioning inhibited ISO-induced apoptosis. (A) The TUNEL-positive cells were shown by the immunohistochemistry method (brown reactions). Dark brown staining indicates TUNEL-positive nuclei. (B) Software analysis for pixel-based intensity for brown reactions (representing positive reaction apoptotic cells) in different sections from different groups in 1 180 μm × 1 180 μm of tissue. ($C_{1,2,3}$) The percent of TUNEL-positive cells ($n = 3$ rats/each group). Consistently, the percentages of TUNEL-positive nuclei were lesser in MIIT + ISO and HIIT + ISO groups compared to the ISO group. Sedentary control (control), (ISO)-induced pathological cardiac remodeling (ISO), moderate intensity of aerobic interval training (MIIT), high intensity of aerobic interval training (HIIT), moderate intensity of aerobic interval training + ISO (MIIT + ISO) and high intensity of aerobic interval training + ISO (HIIT + ISO). Significance was determined by One-Way ANOVA followed by a Tukey Post-hoc test ($C_{1,2}$). Data were analyzed using the Student's *t*-test (C_3). All data are presented in the mean ± *SEM*.

and to explore the protective effects of MIIT and HIIT. Observations revealed massive necrosis, edema, and immune cell infiltration associated with irregular myocardial orientation and severe hemorrhage. The results obtained from MIIT + ISO and HIIT + ISO groups demonstrated that these exercises regimens can protect cardiac tissue from ISO-induced disorders. However, both MIIT and HIIT were found to protect cardiac tissue from these ISO-induced disorders, with HIIT showing more pronounced protective effects.

ISO triggers the production of excessive reactive oxygen species (ROS), leading to a decrease in antioxidants and an increase oxidative stress, which cause alterations in cardiac metabolism, progressive cardiac remodeling and myocardial injury.[4] Oxidative stress, caused by an overproduction of ROS that can't be adequately neutralized by the body's antioxidant systems, plays a crucial role in the development and progression of cardiac remodeling.[37,38] It has been demonstrated that an imbalanced ratio of oxyradicals to antioxidants can negatively affect cardiac function, and this imbalance is closely associated with the functioning of the GSH/GSSH and NADPH/NADP networks.[39,40] The relative ratio of GSSG to glutathione (GSH) is used as a marker of oxidative stress index (OSI), as GSH is an important scavenger of ROS in cardiac tissue.[41] GSH can also act as an antioxidant in association with glutathione peroxidase (GPx) to decrease lipid hydroperoxides.[41,42] Previous studies have shown that exercise training and physical activities are able to boost the cardiac antioxidant system by decreasing the lipid peroxidation ratio and amplifying the enzymatic and nonenzymatic antioxidant statuses.[43–45] Taking these findings into consideration, an analysis of the changes have been conducted in cardiac TAC, TOS, GSH, and GSSG levels. Additionally, the GSSG/GSH ratio was examined to assess the redox balance before and after ISO induction, both in MIIT and HIIT protocols. Observations revealed a mean decrease in cardiac TAC and an increase in TOS, leading to an altered TOS/TAC ratio and a changed ratio of GSSG to GSH in the ISO group compared to the control rats. The results indicated that the HIIT + ISO groups exhibited well-controlled TOS/TAC ratios, while the MIIT + ISO groups showed

restored GSSG/GSH ratios compared to the ISO groups. These initial findings suggest that AITs preconditioning may contribute to the preservation of the pro-oxidant-antioxidant balance in cardiac tissue following ISO induction.

The Beclin-1 complex is well-established to play a crucial role in generating phosphatidylinositol-3-phosphate (PI3P), which is essential for initiating the nucleation of autophagosomes. Furthermore, Atg7, in collaboration with other proteins, is involved in both the elongation of the autophagosome membrane and the lipid conjugation of LC3-I.[46,47] Ultimately, the free form of LC3-I undergoes conversion to the lipid-conjugated form, LC3-II, completing the formation of the autophagosome.[48] The p62, a specific autophagy cargo reporter, is an autophagy substrate that reflects the autophagy intensity.[49]

The hypothesis that ISO-induced oxidative stress can trigger the overexpression of autophagy stimulators is based on the established association between an imbalanced pro-oxidant-antioxidant balance and autophagy,[50,51] as well as the close relationship between the overexpression of autophagy stimulators and apoptosis.[52,53] This scenario could result in prolonged apoptosis, aponecrosis conditions, and the manifestation of hemorrhage and immune cell infiltration in cardiac tissue. Indeed, ISO does pose a pathological challenge to the heart, and understanding the cellular response to ISO is a critical aspect of the study, providing a novel approach to mitigating the pathological effects of ISO on the heart. The present study aimed to ascertain whether AITs preconditioning could modulate this process by preserving physiological autophagy and inhibiting the progression of autophagy-necrosis pathways. A significant increase was observed in the expression levels of autophagy-related biomarkers (Beclin-1, Atg-7, p62, and LC3I/II), compared to the control rats, providing valuable insights into the potential impact of AITs preconditioning on this process.

The MIIT + ISO, and more effectively the HIIT + ISO group exhibited a rebalancing effect on these biomarkers. Initially, it appears that ISO enhances oxidative autophagy, and MIIT may effectively preserve this condition by maintaining a balanced pro-oxidant-antioxidant system and inhibiting autophagy progression, providing valuable insights. However, despite achieving a controlled pro-oxidant-antioxidant balance, HIIT in the HIIT + ISO group was unable to sustain autophagy progression. However, despite the immunohistochemical analysis findings, the HIIT + ISO rats exhibited higher protein levels of LC3I/II, a hallmark of autophagy, compared to the MIIT-preconditioned group. Interestingly, despite the observed differences in autophagy progression, the HIIT + ISO group displayed more favorable results in terms of apoptotic cell detection, as demonstrated by no significant differences in the TUNEL test and active caspase-3 staining compared to the MIIT + ISO rats. This suggests that the relationship between autophagy and apoptosis in response to different intensity of EP is complex and warrants further investigation.

It is essential to emphasize the pivotal role of regulated autophagy in promoting cell survival by eliminating damaged organelles and/or cellular contents in response to oxidative damage. Moreover, controlled autophagy serves as a mechanism to impede the progression of apoptosis.[54,55] The findings suggest that HIIT (in the HIIT + ISO group), preserved CMs from apoptosis through a regulated autophagy system. Conversely, in the MIIT + ISO group, MIIT protected CMs from ISO-induced apoptosis by maintaining a balanced pro-oxidant-antioxidant system linked with GSH/GSSH relative ratio, potentially inhibiting autophagy and autophagy-related apoptosis.

4.1. Study limitations

The blood pressure results may not be directly applicable to human populations as it was assessed under anesthetic conditions. Furthermore, the study specifically focused on the effects of MIIT and HIIT on ISO-induced PCR. Long-term outcomes, such as functional recovery, long-term survival rates, and other relevant clinical endpoints were not evaluated. Additionally, while the study examined histological alterations, oxidative balance, autophagy, and apoptosis in cardiac tissue, the underlying mechanisms through which MIIT and HIIT exert their effects were not fully elucidated. Further research is required to gain a deeper understanding of the specific molecular pathways involved.

5. Conclusion

The present study suggests that ISO disrupts the pro-oxidant-antioxidant balance and initiates pro-apoptotic autophagy in the cardiac tissue. Both MIIT and HIIT preconditioning could be beneficial in maintaining this balance following ISO induction, with MIIT primarily inhibiting pro-apoptotic autophagy and HIIT promoting pro-survival autophagy. This highlights the complexity of the interplay between exercise, oxidative stress, and autophagy, and underscores the need for further research. MIIT and HIIT can both decrease the negative effects of ISO, with HIIT being more effective in the early stage and MIIT in the later stage. Optimizing exercise protocols could be a promising avenue for therapeutic intervention in conditions characterized by oxidative stress and impaired autophagy. Further research is required to comprehend their underlying mechanisms and optimize the use of MIIT and HIIT for cardiac protection.

Submission statement

All authors have read and agree with the manuscript content. While this manuscript is being reviewed for Sports Medicine and Health Science, it will not be submitted elsewhere for review and publication.

Ethical approval statement

All animals were housed at (23 ± 2) °C under a 12 h dark and 12 h light cycle. Food and water were provided ad libitum during the experimental period. All animal studies and experimental trials used conform to the Directive 2010/63/EU of the European Parliament and were approved and monitored by the ethical committee of laboratory animals, Urmia University (Approval NO: IR-UU-AEC-3/18).

Funding

This research did not receive any specific grant from funding agencies in the public, commercial, or not-for-profit sectors.

Authors' contribution statement

Hakimeh Shahsavarnajand Bonab: Writing – original draft, Methodology, Investigation, Formal analysis, Conceptualization. **Javad Tolouei Azar:** Writing – review & editing, Visualization, Validation, Supervision, Software, Resources, Project administration, Methodology, Investigation, Formal analysis, Data curation, Conceptualization. **Hamid Soraya:** Writing – review & editing, Visualization, Supervision, Project administration, Methodology, Conceptualization, Establishing the animal model. **Akbar Nouri Habashi:** Writing – review & editing, Methodology, Formal analysis, Conceptualization.

Conflict of interest

All authors have no direct or indirect interests that are in direct conflict with the conduction of the study.

Acknowledgement

The present manuscript is derived from a Ph.D. thesis (NO: 11112). The authors wish to extend their gratitude for the scientific support received from the Faculty of Sport Sciences, Urmia University, and the

School of Pharmacy, Urmia University of Medical Sciences. Furthermore, the authors would like to acknowledge the valuable assistance provided by the RASTA special research institute (RSRI) in the laboratory.

References

1. Zuo Z, Ji MY, Zhao K, et al. CD47 deficiency attenuates isoproterenol-induced cardiac remodeling in mice. *Oxid Med Cell Longev*. 2019;2019:7121763. https://doi.org/10.1155/2019/7121763.
2. Azevedo PS, Polegato BF, Minicucci MF, Paiva SA, Zornoff LA. Cardiac remodeling: concepts, clinical impact, pathophysiological mechanisms and pharmacologic treatment. *Arq Bras Cardiol*. 2016;106(1):62–69. https://doi.org/10.5935/abc.20160005.
3. Soraya H, Khorrami A, Garjani A, Maleki-Dizaji N, Garjani A. Acute treatment with metformin improves cardiac function following isoproterenol induced myocardial infarction in rats. *Pharmacol Rep*. 2012;64(6):1476–1484. https://doi.org/10.1016/s1734-1140(12)70945-3.
4. Shanmugam G, Challa AK, Devarajan A, et al. Exercise mediated Nrf2 signaling protects the myocardium from isoproterenol-induced pathological remodeling. *Front Cardiovasc Med*. 2019;6:68. https://doi.org/10.3389/fcvm.2019.00068.
5. Li L, Qi W, Zhu Y, et al. Danlou tablet protects against cardiac remodeling and dysfunction after myocardial ischemia/reperfusion injury through activating AKT/FoxO3a pathway. *J Cardiovasc Transl Res*. 2023;16(4):803–815. https://doi.org/10.1007/s12265-023-10365-x.
6. Wang X, Guo Z, Ding Z, Mehta JL. Inflammation, autophagy, and apoptosis after myocardial infarction. *J Am Heart Assoc*. 2018;7(9):e008024. https://doi.org/10.1161/JAHA.117.008024.
7. Popgeorgiev N, Sa JD, Jabbour L, et al. Ancient and conserved functional interplay between Bcl-2 family proteins in the mitochondrial pathway of apoptosis. *Sci Adv*. 2020;6(40):eabc4149. https://doi.org/10.1126/sciadv.abc4149.
8. Nishida K, Otsu K. Autophagy during cardiac remodeling. *J Mol Cell Cardiol*. 2016;95:11–18. https://doi.org/10.1016/j.yjmcc.2015.12.003.
9. Ding W, Feng H, Li W-j, Liao H-h, Tang Q-z. Research progress on the interaction between autophagy and energy homeostasis in cardiac remodeling. *Front Pharmacol*. 2020;11:587438. https://doi.org/10.3389/fphar.2020.587438.
10. Boťanská B, Dovinová I, Barančík M. The interplay between autophagy and redox signaling in cardiovascular diseases. *Cells*. 2022;11(7):1203. https://doi.org/10.3390/cells11071203.
11. Davidson SM, Adameová A, Barile L, et al. Mitochondrial and mitochondrial-independent pathways of myocardial cell death during ischaemia and reperfusion injury. *J Cell Mol Med*. 2020;24(7):3795–3806. https://doi.org/10.1111/jcmm.15127.
12. Chen H, Chen C, Spanos M, et al. Exercise training maintains cardiovascular health: signaling pathways involved and potential therapeutics. *Signal Transduct Targeted Ther*. 2022;7(1):306. https://doi.org/10.1038/s41392-022-01153-1.
13. Lira VA, Okutsu M, Zhang M, et al. Autophagy is required for exercise training-induced skeletal muscle adaptation and improvement of physical performance. *Faseb J*. 2013;27(10):4184–4193. https://doi.org/10.1096/fj.13-228486.
14. Davos CH. Do we have to reconsider the guidelines for exercise intensity determination in cardiovascular rehabilitation? *Eur J Prev Cardiol*. 2019;26(18):1918–1920. https://doi.org/10.1177/2047487319871870.
15. Quindry JC, Franklin BA. Exercise preconditioning as a cardioprotective phenotype. *Am J Cardiol*. 2021;148:8–15. https://doi.org/10.1016/j.amjcard.2021.02.030.
16. Lennon SL, Quindry JC, French JP, Kim S, Mehta JL, Powers SK. Exercise and myocardial tolerance to ischaemia-reperfusion. *Acta Physiol Scand*. 2004;182(2):161–169. https://doi.org/10.1111/j.1365-201X.2004.01346.x.
17. Quindry JC, Miller L, McGinnis G, et al. Ischemia reperfusion injury, KATP channels, and exercise-induced cardioprotection against apoptosis. *J Appl Physiol(1985)*. 2012;113(3):498–506. https://doi.org/10.1152/japplphysiol.00957.2011.
18. Chowdhury MA, Sholl HK, Sharrett MS, et al. Exercise and cardioprotection: a natural defense against lethal myocardial ischemia–reperfusion injury and potential guide to cardiovascular prophylaxis. *J Cardiovasc Pharmacol Therapeut*. 2019;24(1):18–30. https://doi.org/10.1177/1074248418788575.
19. Ping Z, Qiu W, Yang M, et al. Optimization of different intensities of exercise preconditioning in protecting exhausted exercise induced heart injury in rats. *Sports Med Health Sci*. 2021;3(4):218–227. https://doi.org/10.1016/j.smhs.2021.10.006.
20. Swain DP, Franklin BA. Comparison of cardioprotective benefits of vigorous versus moderate intensity aerobic exercise. *Am J Cardiol*. 2006;97(1):141–147. https://doi.org/10.1016/j.amjcard.2005.07.130.
21. Yamashita N, Hoshida S, Otsu K, Asahi M, Kuzuya T, Hori M. Exercise provides direct biphasic cardioprotection via manganese superoxide dismutase activation. *J Exp Med*. 1999;189(11):1699–1706. https://doi.org/10.1084/jem.189.11.1699.
22. Meng D, Li P, Huang X, Jiang M-H, Cao X-B. Protective effects of short-term and long-term exercise preconditioning on myocardial injury in rats. *Chin J Appl Physiol*. 2017;33(6):531–534. https://doi.org/10.12047/j.cjap.5601.2017.126.
23. McGinnis GR, Ballmann C, Peters B, et al. Interleukin-6 mediates exercise preconditioning against myocardial ischemia reperfusion injury. *Am J Physiol Heart Circ Physiol*. 2015;308(11):H1423–H1433. https://doi.org/10.1152/ajpheart.00850.2014.
24. MacInnis MJ, Gibala MJ. Physiological adaptations to interval training and the role of exercise intensity. *J Physiol*. 2017;595(9):2915–2930. https://doi.org/10.1113/JP273196.
25. Jiang HK, Miao Y, Wang YH, et al. Aerobic interval training protects against myocardial infarction-induced oxidative injury by enhancing antioxidase system and mitochondrial biosynthesis. *Clin Exp Pharmacol Physiol*. 2014;41(3):192–201. https://doi.org/10.1111/1440-1681.12211.
26. Kemi OJ, Ellingsen Ø, Ceci M, et al. Aerobic interval training enhances cardiomyocyte contractility and Ca2+ cycling by phosphorylation of CaMKII and Thr-17 of phospholamban. *J Mol Cell Cardiol*. 2007;43(3):354–361. https://doi.org/10.1016/j.yjmcc.2007.06.013.
27. Naderi N, Hemmatinafar M, Gaeini AA, et al. High-intensity interval training increase GATA4, CITED4 and c-Kit and decreases C/EBPβ in rats after myocardial infarction. *Life Sci*. 2019;221:319–326. https://doi.org/10.1016/j.lfs.2019.02.045.
28. Li B, Liang F, Ding X, et al. Interval and continuous exercise overcome memory deficits related to β-Amyloid accumulation through modulating mitochondrial dynamics. *Behav Brain Res*. 2019;376:112171. https://doi.org/10.1016/j.bbr.2019.112171.
29. Petrosino JM, Heiss VJ, Maurya SK, et al. Graded maximal exercise testing to assess mouse cardio-metabolic phenotypes. *PLoS One*. 2016;11(2):e0148010. https://doi.org/10.1371/journal.pone.0148010.
30. Elshazly A, Khorshid H, Hanna H, Ali A. Effect of exercise training on heart rate recovery in patients post anterior myocardial infarction. *Egypt Heart J*. 2018;70(4):283–285. https://doi.org/10.1016/j.ehj.2018.04.007.
31. Adams V, Reich B, Uhlemann M, Niebauer J. Molecular effects of exercise training in patients with cardiovascular disease: focus on skeletal muscle, endothelium, and myocardium. *Am J Physiol Heart Circ Physiol*. 2017;313(1):H72–H88. https://doi.org/10.1152/ajpheart.00470.2016.
32. Zhang YM, Lu Y, Tang Y, et al. The effects of different initiation time of exercise training on left ventricular remodeling and cardiopulmonary rehabilitation in patients with left ventricular dysfunction after myocardial infarction. *Disabil Rehabil*. 2016;38(3):268–276. https://doi.org/10.3109/09638288.2015.1036174.
33. Maessen MF, Eijsvogels TM, Stevens G, van Dijk AP, Hopman MT. Benefits of lifelong exercise training on left ventricular function after myocardial infarction. *Eur J Prev Cardiol*. 2017;24(17):1856–1866. https://doi.org/10.1177/2047487317728765.
34. Quindry J, French J, Hamilton K, Lee Y, Mehta JL, Powers S. Exercise training provides cardioprotection against ischemia-reperfusion induced apoptosis in young and old animals. *Exp Gerontol*. 2005;40(5):416–425. https://doi.org/10.1016/j.exger.2005.03.010.
35. Xing Y, Yang SD, Wang MM, Feng YS, Dong F, Zhang F. The beneficial role of exercise training for myocardial infarction treatment in elderly. *Front Physiol*. 2020;11:270. https://doi.org/10.3389/fphys.2020.00270.
36. Metias E, Aboelmaaty N, Hussein A, Abdallah E, Abdelaziz A. Modulation of ECG, myocardial oxidative stress markers and connexion 43 expression by ascorbic acid and ferulic acid in isoproterenol-induced myocardial infarction in rats. *Biochem Physiol*. 2016;5(210):2. https://doi.org/10.4172/2168-9652.1000210.
37. Takimoto E, Kass DA. Role of oxidative stress in cardiac hypertrophy and remodeling. *Hypertension*. 2007;49(2):241–248. https://doi.org/10.1161/01.HYP.0000254415.31362.a7.
38. Harvey A, Grieve D. Reactive oxygen species (ROS) signaling in cardiac remodeling and failure. In: Laher I, ed. *Systems Biology of Free Radicals and Antioxidants*. Springer; 2014:951–992. https://doi.org/10.1007/978-3-642-30018-9_50.
39. Shah AKBS, Elimban V, Dhalla NS. Oxidative stress as a mechanism for functional alterations in cardiac hypertrophy and heart failure. *Antioxidants*. 2021;10(6):931. https://doi.org/10.3390/antiox10060931.
40. Tangvarasittichai S. Oxidative stress, insulin resistance, dyslipidemia and type 2 diabetes mellitus. *World J Diabetes*. 2015;6(3):456–480. https://doi.org/10.4239/wjd.v6.i3.456.
41. Kurian GA, Rajagopal R, Vedantham S, Rajesh M. The role of oxidative stress in myocardial ischemia and reperfusion injury and remodeling: revisited. *Oxid Med Cell Longev*. 2016;2016:1656450. https://doi.org/10.1155/2016/1656450.
42. Das P, Nutan KK, Singla-Pareek SL, Pareek A. Oxidative environment and redox homeostasis in plants: dissecting out significant contribution of major cellular organelles. *Front Environ Sci*. 2015;2:70. https://doi.org/10.3389/fenvs.2014.00070.
43. Lu K, Wang L, Wang C, Yang Y, Hu D, Ding R. Effects of high-intensity interval versus continuous moderate-intensity aerobic exercise on apoptosis, oxidative stress and metabolism of the infarcted myocardium in a rat model. *Mol Med Rep*. 2015;12(2):2374–2382. https://doi.org/10.3892/mmr.2015.3669.
44. Lu Y, Wiltshire HD, Baker JS, Wang Q. Effects of high intensity exercise on oxidative stress and antioxidant status in untrained humans: a systematic review. *Biology*. 2021;10(12):1272. https://doi.org/10.3390/biology10121272.
45. Jia D, Hou L, Lv Y, Xi L, Tian Z. Postinfarction exercise training alleviates cardiac dysfunction and adverse remodeling via mitochondrial biogenesis and SIRT1/PGC-1α/PI3K/Akt signaling. *J Cell Physiol*. 2019;234(12):23705–23718. https://doi.org/10.1002/jcp.28939.
46. Ryter SW, Mizumura K, Choi AM. The impact of autophagy on cell death modalities. *Int J Cell Biol*. 2014;2014:502676. https://doi.org/10.1155/2014/502676.
47. Runwal G, Stamatakou E, Siddiqi FH, Puri C, Zhu Y, Rubinsztein DC. LC3-positive structures are prominent in autophagy-deficient cells. *Sci Rep*. 2019;9:10147. https://doi.org/10.1038/s41598-019-46657-z.
48. Akbar Gharehbagh S, Tolouei Azar J, Razi M. ROS and metabolomics-mediated autophagy in rat's testicular tissue alter after exercise training; Evidence for exercise intensity and outcomes. *Life Sci*. 2021;277:119585. https://doi.org/10.1016/j.lfs.2021.119585.
49. Liu WJ, Ye L, Huang WF, et al. p62 links the autophagy pathway and the ubiqutin–proteasome system upon ubiquitinated protein degradation. *Cell Mol Biol Lett*. 2016;21:29. https://doi.org/10.1186/s11658-016-0031-z.

50. Navarro-Yepes J, Burns M, Anandhan A, et al. Oxidative stress, redox signaling, and autophagy: cell death versus survival. *Antioxidants Redox Signal*. 2014;21(1):66–85. https://doi.org/10.1089/ars.2014.5837.
51. Ornatowski W, Lu Q, Yegambaram M, et al. Complex interplay between autophagy and oxidative stress in the development of pulmonary disease. *Redox Biol*. 2020;36:101679. https://doi.org/10.1016/j.redox.2020.101679.
52. Wärri A, Cook KL, Hu R, et al. Autophagy and unfolded protein response (UPR) regulate mammary gland involution by restraining apoptosis-driven irreversible changes. *Cell Death Dis*. 2018;4:40. https://doi.org/10.1038/s41420-018-0105-y.
53. Li P, Ma R, Dong L, et al. Autophagy impairment contributes to PBDE-47-induced developmental neurotoxicity and its relationship with apoptosis. *Theranostics*. 2019;9(15):4375–4390. https://doi.org/10.7150/thno.33688.
54. Das G, Shravage BV, Baehrecke EH. Regulation and function of autophagy during cell survival and cell death. *Cold Spring Harbor Perspect Biol*. 2012;4(6):a008813. https://doi.org/10.1101/cshperspect.a008813.
55. Filomeni G, De Zio D, Cecconi F. Oxidative stress and autophagy: the clash between damage and metabolic needs. *Cell Death Differ*. 2015;22(3):377–388. https://doi.org/10.1038/cdd.2014.150.